sustainability

MDPI

Article

Research on the Correlation Mechanism Between Complex Slopes of Mountain City Roads and the Real Driving Emission of Heavy-Duty Diesel Vehicles

Gangzhi Tang *, Dong Liu, Jiajun Liu and Xuefei Deng

College of Mechatronics & Vehicle Engineering, Chongqing Jiaotong University, Chongqing 400074, China; dongliu01@outlook.com (D.L.); 622230990017@mails.cqjtu.edu.cn (J.L.); 622230040038@mails.cqjtu.edu.cn (X.D.)
* Correspondence: 990201400028@cqjtu.edu.cn; Tel.: +86-13658340960

Abstract: This research proposed the method of using cumulative positive and negative elevation increment indicators based on road segment to identify the slope characteristics of mountain city roads. Furthermore, it proposed the adoption of these indicators, combined with driving dynamics and emission theory, to analyze the correlation mechanism between the road slope and the actual driving fuel consumption and emissions. Three routes with different slope characteristics were selected in the mountain city of Chongqing, and six road driving tests were conducted using a Class N2 heavy-duty diesel vehicle. Finally, a comprehensive and in-depth study on fuel consumption and emission characteristics was carried out. The results show that the cumulative positive and negative elevation increment indicators based on road segment can correctly identify the complex slope characteristics of mountain city roads. Moreover, using the above indicators, the research method based on the theory of driving dynamics and emission successfully revealed the correlation mechanism between the slope of mountain city roads and the fuel consumption and emissions. Overall, the changes in fuel consumption factor and pollutants CO, NO_X, and PN are positively correlated with the change in slope. The increase in slope leads to a rise in load, thereby increasing the required power, fuel consumption, and rich combustion conditions, ultimately leading to an increase in pollutants. It should be noted that driving dynamics also affect fuel consumption and emissions, leading to the specific rate of change between slope and fuel consumption not being consistent and a significant increase in the PN (Particulate Number) on some road sections. In addition, exhaust gas temperature may have a certain impact on emissions.

Keywords: PEMS; cumulative elevation increment; emission factor; mountain city roads; correlation mechanism

check for updates

Academic Editor: Carlos Llopis-Albert

Received: 26 November 2024
Revised: 27 December 2024
Accepted: 9 January 2025
Published: 13 January 2025

Citation: Tang, G.; Liu, D.; Liu, J.; Deng, X. Research on the Correlation Mechanism Between Complex Slopes of Mountain City Roads and the Real Driving Emission of Heavy-Duty Diesel Vehicles. *Sustainability* **2025**, *17*, 554. https://doi.org/10.3390/su17020554

Copyright: © 2025 by the authors. Licensee MDPI, Basel, Switzerland. This article is an open access article distributed under the terms and conditions of the Creative Commons Attribution (CC BY) license (https://creativecommons.org/licenses/by/4.0/).

1. Introduction

With the rapid development of China's economy, the demand for motor vehicles has been increasing. The total number of motor vehicles increased from 16 million in 2000 to 395 million in 2021, which is a 24-fold increase during this period [1]. Although the government's emission standards for motor vehicles are more stringent year by year, the emissions continue to rise significantly in the face of the continuous growth of motor vehicle ownership. Motor vehicle emissions have become a major contributor to environmental pollution [2]. In European countries, road transportation emissions account for about 40% of NO_X emissions, with the main share coming from passenger and freight transportation [3].

In China's traffic-intensive urban areas, vehicle emissions account for about 70% of NO_X emissions, mainly from diesel vehicles [4].

Vehicle emissions greatly contribute to the formation of secondary air pollutants, including fine particulate matter (PM2.5) and ozone, which have been found to significantly increase mortality and cause other health effects [5–7]. Controlling vehicle emissions has become a major challenge nowadays.

Currently, the testing of vehicle emissions mainly includes tests conducted on chassis dynamometer test benches in fixed laboratories and actual road driving pollutant emission tests carried out using Portable Emission Measurement Systems (PEMSs). Despite the good repeatability and the use of high-precision measurement equipment, laboratory tests cannot accurately reproduce actual driving conditions. This leads to discrepancies between bench test results and real-world emissions, limiting their reliability [8]. For this reason, scholars have proposed test cycles that are closer to real driving conditions, and cycle tests show that the accuracy of emission results in reflecting real emissions has improved to a certain extent [9–11]. Although the laboratory certification cycle conditions are becoming more and more consummate and comprehensive, there is still a significant difference between the emissions of vehicles under real road conditions and those under laboratory bench test conditions [12]. Parameters involved in bench tests, such as temperature range, driving dynamics, acceleration and deceleration frequency, road slope, etc., differ from those during real driving, resulting in actual driving emissions often being greater than bench test results. Real road driving tests based on Portable Emission Measurement Systems are becoming increasingly important. They can monitor and analyze various parameters during the actual driving process of vehicles in real time, which is more conducive to obtaining emission results that conform to the actual situation [13–15].

Liu et al. conducted a comparative study of various PEMS and chassis dynamometer tests on a laboratory bench [16]. The results showed that the CO, NO_X, CO_2, and HC measured by PEMS exhibited a high consistency with those obtained from the chassis dynamometer. A comparison of different PEMS test results also demonstrated that PEMS testing has good stability. Comparative tests conducted by Gallus et al. on laboratory benches indicate that the PEMS test PN (Particulate Number) has good consistency with the chassis dynamometer test PN, suggesting that PEMS can be used for actual road driving tests [17]. Now, real drive emission tests using PEMS have been approved for emission certification to supplement chassis dynamometer tests in many regions [18].

Real driving emission and fuel consumption tests using PEMS indicate that real driving emissions are influenced by operating conditions, driving behavior, environment, and other external factors. Therefore, accurately capturing the real emission characteristics of vehicles becomes very challenging. The study of Gallus et al. confirms that driving style and low-temperature environmental conditions during cold starts have a significant impact on PN [17]. Degraeuwe and Weiss selected seven diesel vehicles to conduct real road driving emission tests based on PEMS. They found that the emission control strategy had a significant impact on NO_X emissions, suggesting that cycle certification tests need to pay further attention to emission control strategies [19]. In the study of Guor et al., three heavy-duty diesel vehicles were tested for emissions and fuel consumption in Beijing using PEMS [20]. The results show that the emission factor has a strong positive correlation with vehicle speed and acceleration. X. Li et al. conducted real road driving tests on NO_X, CO_2, and fuel consumption of three heavy-duty diesel vehicles in Beijing and Chifeng, Inner Mongolia, China, and analyzed the combined effects of SCR, speed, and air–fuel ratio on emissions, confirming that all three factors have an impact on emissions [21]. A study confirms that driving emissions can be reduced by adopting calmer driving behaviors [22]. Research results from Lois et al. confirmed that in addition to driving

behaviors such as deceleration rate, engine speed, and speed having a significant impact on fuel consumption, external factors such as traffic congestion and road slope also directly affect fuel consumption [23]. Zhai et al. have investigated the impact of vehicle driving parameters, engine operating parameters, road slope, and climate weather on road fuel consumption and emissions [24]. They found that all of the above factors affect fuel consumption and emissions. In some literature [25,26], it is shown that road characteristics are often overlooked in laboratory emission tests. Road slope among road characteristics plays an important role in vehicle fuel consumption and emissions of traveling vehicles.

A series of studies has confirmed that the road slope has a significant impact on both the actual driving fuel consumption and emissions. Boriboonsomsin and Barth conducted a comparative study on vehicle fuel economy on hilly and flat routes [27]. The results showed that at a speed maintained at 60 mph, the uphill sections of the hilly route had poor fuel economy, while the downhill sections had the best. The overall fuel economy of the flat route was approximately 15% to 20% higher than that of the hilly route. Slope has a significant effect on fuel consumption. Travesset-Baro et al. developed a model to comparatively analyze the effect of factors such as terrain and driving pattern on fuel consumption of light-duty diesel vehicles and electric vehicles [28]. The results showed that road slope has a significant impact on vehicle driving fuel consumption performance, with the effect of slope on diesel vehicle fuel consumption being more pronounced than its effect on electric vehicle energy consumption. Zhang et al. studied the influence of slopes in hilly terrain on the emissions of heavy-duty vehicles in Taiyuan city [29]. The results show that slope affects driving emissions, and when the slope is between 0–0.5% and 2.5–3.0%, its impact on total emissions is most significant. H. Yang et al. conducted emission tests on motorcycles that meet the Euro 5 standard on urban, suburban, uphill, and downhill routes and studied the impact of slope on emissions [30]. The results showed that the emission factors for all measured pollutants on uphill routes were significantly higher than those on downhill routes, with slope significantly affecting emissions. The relationship between slope and fuel consumption and emissions has become a research hotspot.

Many scholars have conducted research on the relationship between road slope and driving fuel consumption and emissions. Wyatt et al. conducted a driving CO_2 emission test on a Ford Mondeo on a circular road in Leeds, UK. A simple LiDAR (Light Detection And Ranging)-GIS (Geographic Information System) road grade estimation methodology was used to calculate the road grade for each second [31]. A PHEM instantaneous emission model was used to estimate the vehicle CO_2 emissions per second. The results show that road slope has a significant impact on both power output and CO_2. For the same section of road, the increase in CO_2 emissions caused by uphill driving cannot be completely offset by the decrease in CO_2 emissions caused by downhill driving. Murena et al. conducted driving tests on a gasoline passenger car and a scooter in Naples city, Italy [32]. GPS was used to track vehicle position information to calculate the road slope. The results showed that the increase in fuel consumption caused by going uphill was greater than the decrease in fuel consumption caused by descending downhill at similar slopes (+70% vs. −38%), indicating that the higher fuel consumption on uphill sections was not compensated for by the lower fuel consumption on downhill sections. NO_X significantly decreased during descent; however, it increased by less than 10% during ascent. CO had a good correlation with slope changes. Lopp et al. have incorporated road slope data into real-world drive cycles through the American digital elevation model and used NREL's Future Automotive Systems Technology Simulator to simulate the fuel economy of various heavy-duty vehicles on these real-world drive cycles [33]. The results indicate that fuel consumption increases on uphill sections and decreases on downhill sections. The engine efficiency is low when going uphill, resulting in a fuel use penalty for climbing that exceeds the benefits of descending.

For a distance, fuel use penalty by average grade and RMS grade both increase with the latter. Wood et al. also conducted simulation studies using real-world driving cycle data, which showed that the fuel consumption penalty brought about by uphill driving exceeded the benefits of downhill driving [34]. Even for trips with net zero elevation changes, fuel consumption was significantly affected by road slope. It is evident that in order to decipher the influence mechanism of road slope characteristics on actual driving fuel consumption and emission characteristics, it is necessary to fully consider the impact of uphill and downhill features of the road on the latter.

Zachiotis, A. T. and Giakoumis, E. G. created multiple sinusoidal elevation profiles that simulate a vehicle trip between consecutive peaks and valleys with the total net elevation being zero and evaluated the effect of slope on driving performance and emission performance [35]. The results show that there is a noteworthy increase in emissions, even for a zero net elevation trip. As the RMS slope increases, there is a trend towards higher fuel consumption and emissions, but the correlation with the former is poor. The reason for this needs to be further researched. Costagliola et al. conducted real road driving emission tests on two diesel vehicles using PEMS and GPS on urban, suburban, and highway roads [26]. The results showed that the emissions of CO, NO_X, and CO_2 (g/km) were usually highest on urban roads. They also selected suburban roads with significant slope changes, divided the roads into slopes, and conducted a study on the impact of slope on emissions. The results indicated that on these sections of road, carbon dioxide emissions were linearly related to slope, while NO_X was binomially related to road slope. This conclusion is not consistent with those of David W. Wyatt, Fabio Murena, and other literature. Therefore, it is necessary to conduct in-depth research on the intrinsic correlation mechanism between slope and actual fuel consumption and emission characteristics.

Therefore, in view of the complex and changeable mountain city road driving scenarios, this research proposes to deeply explore the influence rules of road slope on driving fuel consumption and emissions based on the theory of driving dynamics and pollutant generation, combined with the cumulative positive and negative elevation increment indicators of each road section. It also reveals the intrinsic correlation mechanism between the road slope of mountainous cities and driving fuel consumption and emissions.

2. Methodology

2.1. Test Contents

2.1.1. Actual Road PEMS Test

In the mountain city of Chongqing, China, three PEMS test routes with different slope characteristics were developed. Two complete PEMS tests were conducted on each route using an N2 class heavy-duty diesel vehicle that meets the National VI emission standards, totaling six complete PEMS tests. Each test was strictly conducted according to the actual road test standard procedures in China National VI heavy-duty vehicles, and instantaneous data were recorded through the Portable Emission Measurement System AVL-MOVE in the test process. The fuel used in each test should be the same, the vehicle load should be the same, and the status of the vehicle's auxiliary systems, such as air conditioning, should remain consistent. To avoid the influence of driving behavior (driving habits) on the test results, the same driver should be selected for each test. In addition, according to the PEMS standard test procedure, after eliminating the engine work during the cold start stage, the engine work required during the PEMS test process needs to meet 4–7 times the WHTC cycle work.

2.1.2. Laboratory C-WTVC Cycle Test

Based on the C-WTVC cycle applicable to N2 class heavy-duty vehicles, three vehicle fuel consumption and emission tests were conducted on the same vehicle using a laboratory chassis dynamometer. The tests were strictly carried out in accordance with the fuel consumption measurement producer of heavy-duty vehicles in China's National VI standard GB/27840-2011. During the test process, instantaneous data were recorded through a Portable Emission Measurement System, AVL-MOVE. After the vehicle and testing equipment were installed, the drum was started, and the engine was warmed up first. Only after the engine coolant temperature of the vehicle reached the standard requirements could the formal test begin. In order to minimize the impact of environmental differences on the results of the two types of experiments, the temperature and humidity of the laboratory tests were maintained at the average values of the environmental temperature and humidity during the PEMS tests. This approach ensures that the environmental conditions of the two types of experiments are kept as similar as possible. Therefore, when comparing the results of C-WTVC cycle tests with PEMS test results, the influence of environmental factors, such as temperature and humidity, on the test results can be ignored.

2.1.3. Test Vehicle

This research selects a representative N2 class heavy-duty diesel truck that meets the National VI emission standards, with specific parameters as shown in Table 1. The engine is a diesel engine with a displacement of 2499 cm^3, maximum power of 110 kW, cycle work of 9.5 kW·h, and maximum allowable total mass of 4485 kg. The cycle work is the effective work output of the engine in the World Harmonized Transient Cycle test. The exhaust after-treatment system integrates EGR (Exhaust Gas Recirculation), DOC (Diesel Oxidation Catalyst), DPF (Diesel Particulate Filter), SCR (Selective Catalytic Reduction), and ASC (Ammonia Slip Catalyst).

Table 1. Main technical parameters of the test vehicle.

Vehicle Type	N2
Engine displacement/cm^3	2499
Maximum power/kW	110
Engine cycle power/kW·h	9.5
Tail gas post-treatment system	DOC + SCR + ASC + DPF
Injection way	High-pressure common rail
Maximum allowable total mass/kg	4485
Mileage traveled/km	2000

2.1.4. Test Equipment and Installation

The portable emission measurement equipment used in this experiment is the AVL-MOVE vehicle exhaust portable emission detection equipment. Prior to the experiment, the equipment was calibrated, and all tests were conducted within the valid period of the device's use. The equipment integrates a gas test detection module, a PN particulate matter detection module, an exhaust flow meter (EFM), a temperature and humidity detector, and GPS, as well as the control unit and power supply. The NO_X content in the exhaust can be measured by the NDUV (Non-dispersive Ultraviolet) analyzer, while the CO content in the exhaust can be measured by the NDIR (non-dispersive infrared) analyzer, with both measurement units being ppm. PN refers to the particulate number of exhaust pollutant, with a unit of "#/km". During the test in this research, the AVL PN module was adopted to measure particle number. The AVL PN module uses a DC principle to measure particle number. The EFM can measure the instantaneous emission of exhaust.

GPS can record instantaneous altitude, longitude and latitude, and vehicle speed, while the temperature and humidity sensor records the instantaneous temperature and humidity of the environment. In addition, during the experiment, a portable battery pack should also be carried to provide a DC power supply voltage of 24 V for the PEMS equipment (including control computer, pollutant testing unit, EFM, temperature and humidity sensor, GPS). The schematic diagram of equipment installation is shown in Figure 1.

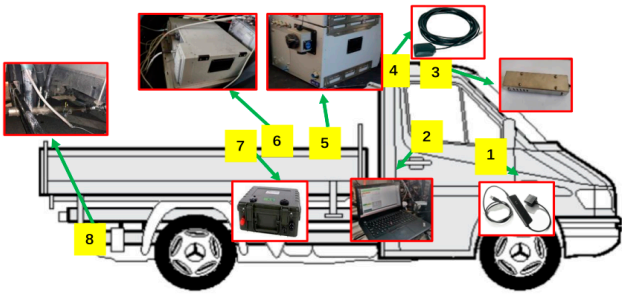

Figure 1. PEMS installation diagram. 1. OBD communication connection; 2. Control computer; 3. Temperature and humidity sensor; 4. GPS; 5. AVL-MOVE-PN unit; 6. AVL-MOVE-gas unit; 7. The battery; 8. Exhaust flow meter.

The EFM is installed on the exhaust pipe of the test vehicle. The connection device between the EFM and the exhaust pipe must not adversely affect the operation of the engine or the exhaust after-treatment system. The gas analysis module, particulate matter analysis module, power supply, gas tank (standard gas and zero gas), etc., are all fixed to the vehicle with straps to prevent damage to the test equipment caused by poor road conditions in the test, leading to inaccurate test measurement results. The emergency switch and control computer are both placed next to the tester so that the tester can observe various test data and control and record any emergencies that occur in the equipment. The weather station and global positioning system are installed on the roof of the vehicle as much as possible to detect more accurate external environmental conditions and ensure good satellite reception signals. Their installation should not affect the normal operation of the vehicle as much as possible.

2.1.5. Test Routes

In this research, three PEMS test routes with different slope characteristics were developed. Routes 1 and 3 are both located in Yubei District, Chongqing City, China, starting from the China Automotive Engineering Research Institute. Route 2 is located in Shuangfu District, Chongqing City, China. The satellite images of the test routes are shown in Figure 2. The route information is shown in Table 2, where 1 and 2 in parentheses represent the first and second trials on the same route.

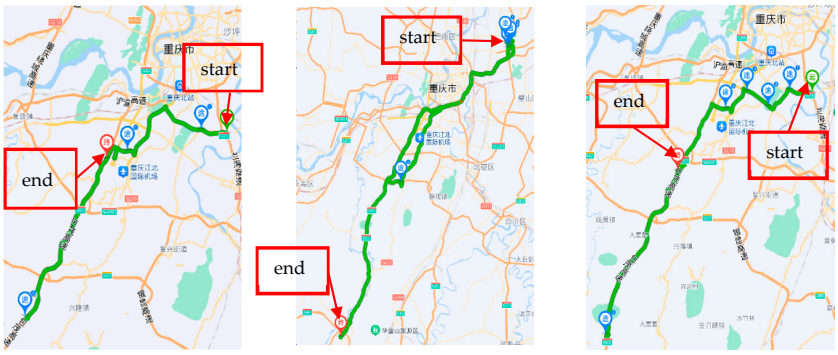

(**a**) Route 1 (**b**) Route 2 (**c**) Route 3

Figure 2. Test road map.

Table 2. Route information.

Test Number	R1(1)	R1(2)	R2(1)	R2(2)	R3(1)	R3(2)	Mean Value	Standard Deviation
The total time/min	161.0	161.4	165.9	176.4	164.0	162.0	165.1	5.3
Total mileage/km	124.4	123.9	130.6	134.5	129.1	129.0	128.6	3.6
Altitude of starting point/m	289.7	289.9	378.6	383.1	291.3	305.3	323.0	41.3
Terminal altitude/m	280.8	278.6	299.9	332.0	336.4	328.2	309.3	24.0
Altitude difference between starting and ending point/m	8.9	11.4	78.7	51.1	45.1	22.8	36.3	24.7
Mean altitude/m	284.0	286.5	318.9	318.9	344.5	343.6	316.0	24.1

2.2. Data Processing Method

In accordance with the requirements of China's National VI regulations of heavy-duty commercial vehicles, the work-based window method is used to process fuel consumption and emission data on the whole trip PEMS test. Due to the long duration of a single work-based window and the fact that power thresholds are used in the National VI standards as a criterion for the validity of work-based windows, it is not possible to calculate pollutant emission using this method for short-term actual road test data. Therefore, this paper will use the cumulative averaging method to process emission and fuel consumption data on the road segment of the PEMS test.

3. Results and Discussion

3.1. Comparative Analysis of C-WTVC and PEMS Results

Based on the instantaneous data read by the vehicle OBD during the test, after eliminating the abnormal data points, the instantaneous fuel consumption and work done were accumulated to obtain the total fuel consumption and total work of the on-road PEMS cycle test and the C-WTVC cycle test in the laboratory. The specific fuel consumption is the ratio of cumulative fuel consumption to cumulative work done. In order to reduce random error, in the study, the average value of two PEMS tests was taken as the specific fuel consumption result of the PEMS test, and the average value of the three laboratory C-WTVC cycle tests was taken as the specific fuel consumption result of the C-WTVC cycle test. The work of the engine is calculated by the test torque and speed.

Table 3 shows that the results of the two PEMS tests are essentially consistent, and the specific fuel consumption of the two tests only differ by 6.7 g/(kW·h). The test results of the three C-WTVC tests also differ slightly, and the cycle work of the three C-WTVC cycle tests is all 9.9 kW·h. The above data indicate that both the on-road PEMS tests and the C-WTVC cycle tests under laboratory conditions have good repeatability.

Table 3. Statistical table of fuel consumption test results.

Test	PEMS		C-WTVC		
	R3(1)	R3(2)	Cycle 1	Cycle 2	Cycle 3
Cumulative fuel consumption/g	12,443.4	11,654.6	2132.5	2133.5	2154.2
Total energy/kW·h	53.1	51.2	9.9	9.9	9.9
Specific fuel consumption g/(kW·h)	234.3	227.6	215.4	215.5	217.6
Average value g/(kW·h)	231.0			216.2	

The table also shows that the specific fuel consumption of the PEMS test is 6.8% higher than that of the C-WTVC test. Vehicle fuel consumption is related to engine work. According to the automobile power balance equation, the amount of engine work is determined by air resistance, rolling resistance, acceleration resistance, and slope resistance

during driving. The environmental temperature and humidity during the two tests are basically consistent, eliminating the influence of environmental factors. During the actual road operation of the PEMS test, its working conditions are more complex. Influenced by actual road slope and traffic factors, the slope resistance and acceleration resistance of vehicles on actual roads differ significantly from those in laboratory conditions. At the same time, the driving dynamics characteristics of vehicles under actual road conditions change drastically. Both factors lead to a higher specific fuel consumption in the PEMS test compared to the C-WTVC test. In addition, other factors will also bring differences in fuel consumption, such as the installation of weather stations and GPS.

Table 4 shows that the difference in CO specific emission is relatively small between the two PEMS tests, while NO_X and PN exhibit significant differences. In the three C-WTVC cycle tests, the differences in CO and PN specific emissions are relatively small, whereas NO_X shows a considerable difference. Overall, both tests' emission results demonstrate a certain degree of repeatability.

Table 4. Statistical table of specific emission results.

Test	PEMS		C-WTVC		
	R3(1)	R3(2)	Cycle 1	Cycle 2	Cycle 3
CO g/(kW·h)	0.40	0.42	0.42	0.47	0.50
NO_X g/(kW·h)	0.03	0.05	0.01	0.03	0.03
PN #/(kW·h)	9.12×10^{10}	1.22×10^{11}	2.18×10^{10}	2.06×10^{10}	2.27×10^{10}

The various pollutant specific emissions in the two sets of experiments shown in Figure 3 exhibit differences. Figure 3a shows that the full-trip CO specific emission in the PEMS experiment is 10.9% lower than that in the laboratory C-WTVC experiment. However, Figure 3b,c show that the NO_X and PN specific emissions in the PEMS experiment are higher than those in the laboratory C-WTVC experiment, with the former being 71.4% and 393.1% higher, respectively. Pollutants are primarily related to the working state of the engine (the conversion efficiency of the exhaust treatment device is good when operating at high temperatures). CO is produced due to incomplete combustion of fuel, often occurring when the vehicle load increases (such as during uphill or acceleration), leading to an increase in the amount of fuel that is not completely burned. NO_X and PN are mainly generated when the engine's working conditions are less than ideal (such as localized hypoxia and higher temperatures). Therefore, it is speculated that the differences in specific emissions of CO, NO_X, and PN may be related to road slope and driving dynamics.

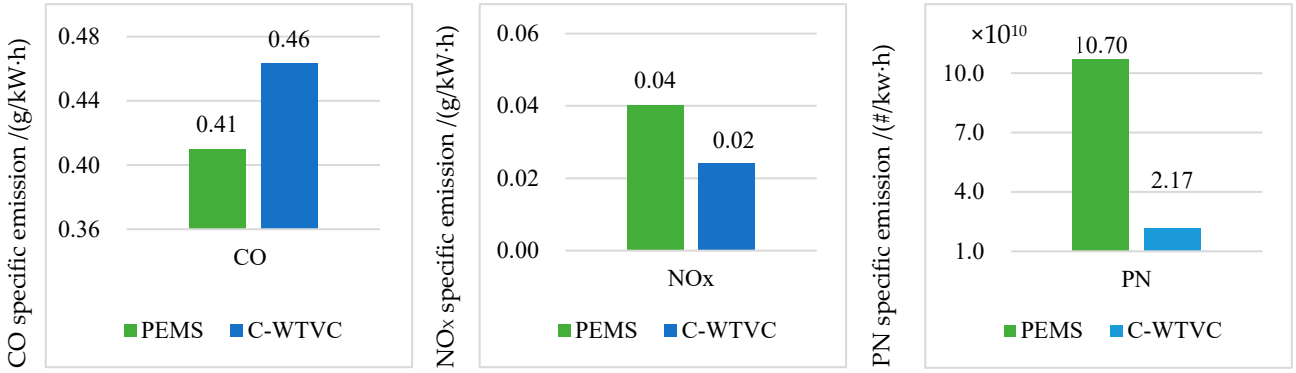

(**a**) CO (**b**) NOx (**c**) PN

Figure 3. Pollutant specific emission statistics of PEMS and C-WTVC.

In summary, road slope is an important factor that caused the difference between the two experimental results. Therefore, it is necessary to conduct in-depth research on the impact mechanism of road slope on PEMS test emissions and fuel consumption.

3.2. Study on the Correlation Mechanism Between Mountain City Road Slopes and Emissions and Fuel Consumption in PEMS Tests

In the current standard for actual road tests of heavy-duty diesel vehicles in China, "Cumulative elevation increment" is used as an important indicator to evaluate road slope. In order to deeply explore the correlation mechanism between the slope of mountain city roads and the fuel consumption and pollutant emissions of heavy-duty diesel vehicles, statistics were collected on the cumulative positive and negative elevation increments from the full trip and each section of six PEMS tests, and the effects of uphill and downhill on the actual road driving emissions and fuel consumption of heavy-duty diesel vehicles were analyzed.

3.2.1. Definition and Statistics of Cumulative Elevation Increment

The PEMS test uses GPS to obtain the vehicle's speed, position, and elevation, with a collection frequency of 1 Hz. By collecting the vehicle's elevation per second through GPS, the cumulative elevation increment of the test route can be calculated. The cumulative positive elevation increment can effectively reflect the uphill amount during the PEMS test. To count the downhill amount, this study proposes the concept of "cumulative negative elevation increment". The following text introduces the definition and statistical methods of cumulative positive elevation increment and cumulative negative elevation increment in vehicle PEMS tests.

The cumulative positive elevation increment is the integral of the positive slope after data processing, reflecting the uphill amount of the entire test route. The cumulative negative elevation increment is the integral of the negative slope after data processing, used to reflect the downhill amount of the entire test route, both in units of m/100 km. The calculation methods of cumulative positive and negative elevation increments are the same. They are roughly divided into two steps: Firstly, the original data with large errors are corrected through the global map module built into the testing system. Then, the road slope is integrated. The specific calculation steps are as follows:

- Screening of measured data and verification of integrity

Check the integrity of the instantaneous elevation data and reasonably interpolate missing data. Interpolation is carried out against high-precision graphic data. And correct the original data: when $| h_{GPS}(t) - h_{map}(t) | > 40$ m, elevation correction should be performed to make $h(t) = h_{map}(t)$, where $h(t)$ represents the vehicle elevation at data point t for data screening and correction, $h_{GPS}(t)$ represents the instantaneous vehicle elevation measured by GPS at data point t, and $h_{map}(t)$ represents the vehicle elevation at data point t based on contour topographic maps.

- Screening and correction of instantaneous vehicle elevation

The elevation obtained by GPS is corrected to the contour topographic map with a deviation of no more than 40 m. If the elevation $h(t)$ during the test satisfies $| h(t) - h(t-1) | > (v(t)/3.6 \times \sin 45^\circ)$, then the elevation correction needs to be corrected as follows: $h_{corr}(t) = h_{corr}(t-1)$. Here, $h(t)$ represents the elevation at data point t after incremental screening and correction, $h(t-1)$ represents the elevation at data point $t-1$ after incremental screening and correction, $v(t)$ represents the vehicle velocity at data point t, $h_{corr}(t)$ represents the corrected instantaneous elevation at data point t, and $h_{corr}(t-1)$ represents the corrected instantaneous elevation at data point $t-1$. After completing the data correction, a valid dataset of elevation is obtained, which is subsequently used to

calculate the cumulative elevation increment. As shown in Figure 4, it displays the curve of instantaneous elevation changes after smooth processing in the experiment.

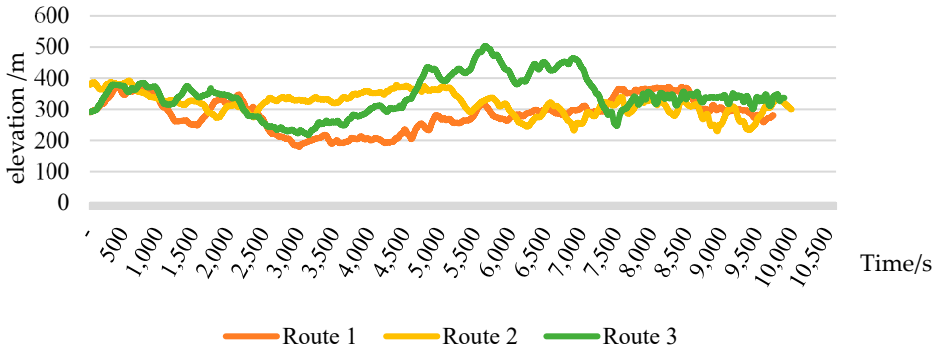

Figure 4. Instantaneous elevation change curve.

- Creating a uniform spatial resolution

The total driving distance $d_{tot}[m]$ should be the sum of the instantaneous distance d_i, according to the following formula to calculate the instantaneous distance d_i:

$$d_i = \frac{v_i}{3.6}$$

where: d_i—instantaneous distance, m;

v_i—instantaneous vehicle speed, km/h.

The cumulative elevation increment is calculated from the first measurement $d(0)$, with a constant spatial resolution of 1 m. Discrete data points at a resolution of 1 m refer to path points characterized by specific distance values d (e.g., 0 m, 1 m, 2 m, 3 m, ...) and their corresponding elevation $h(d)[m]$. The elevation at each discrete path point d is calculated from the interpolated instantaneous elevation $h_{corr}(t)$.

$$h_{int}(d) = h_{corr}(0) + \frac{h_{corr}(1) - h_{corr}(0)}{d_1 - d_0} \times (d - d_0)$$

where: $h_{int}(d)$—interpolated elevation at the discrete path point d, m

$h_{corr}(0)$—corrected elevation before the path point d, m

$h_{corr}(1)$—corrected elevation after the path point d, m

d—cumulative travel distance before the discrete path point d, m

d_0—cumulative travel distance measured before the path point d, m

d_1—cumulative travel distance measured after the path point d, m

- Smooth processing of the additional data

The elevation data obtained for each discrete path point is smoothed in two steps; d_a and d_e represent the first and last data point, respectively, and the first smoothing is performed as follows:

If d $\leq$ 200 m

$$road_{grade,1}(d) = \frac{h_{int}(d + 200) - h_{int}(d_a)}{(d + 200)}$$

If 200 m < $d < d_e - 200$ m

$$road_{grade,1}(d) = \frac{h_{int}(d + 200) - h_{int}(d - 200)}{(d + 200) - (d - 200)}$$

If $d \geq d_e - 200$ m

$$road_{grade,1}(d) = \frac{h_{int}(d_e) - h_{int}(d-200)}{d_e - (d-200)}$$

$$h_{int,sm,1}(d) = h_{int,sm,1}(d-1) + road_{grade,1}(d)$$

$d = d_a + 1$ to d_e

$$h_{int,sm,1}(d_a) = h_{int}(d_a) + road_{grade,1}(d_a)$$

where: $road_{grade,1}(d)$—road slope at the discrete path point d after the first smooth treatment, m/m

$h_{int}(d)$—interpolated elevation of the discrete path point d, m

$h_{int,sm,1}(d)$—interpolated elevation of the discrete path point d after the first smooth treatment, m

d—cumulative travel distance of the discrete path points, m

d_a—reference path point at the 0 m distance

d_e—cumulative travel distance before the last discrete path point, m.

The second smoothing is performed as follows:

If $d \leq 200$ m

$$road_{grade,2}(d) = \frac{h_{int,sm,1}(d+200) - h_{int,sm,1}(d_a)}{(d+200)}$$

If 200 m < d < $d_e - 200$ m

$$road_{grade,2}(d) = \frac{h_{int,sm,1}(d+200) - h_{int,sm,1}(d-200)}{(d+200) - (d-200)}$$

If $d \geq d_e - 200$ m

$$road_{grade,2}(d) = \frac{h_{int,sm,1}(d_e) - h_{int,sm,1}(d-200)}{d_e - (d-200)}$$

where: $road_{grade,2}(d)$—road slope at the discrete path point d after the second smooth treatment, m/m

$h_{int,sm,1}(d)$—interpolated elevation of the discrete path point d after the first smooth treatment, m

d—cumulative distance traveled at the discrete path points, m

d_a—reference path point at the 0 m distance

d_e—cumulative travel distance before the last discrete path point, m.

- Final calculation results

The cumulative positive and negative elevation increments of the trip are calculated by integrating the positive or negative road slopes, i.e., $road_{grade,2}(d)$, which have been interpolated forward and smoothed. The result should be dimensionless by dividing by the total test distance d_{tot} and expressed in terms of cumulative elevation increment (m) per hundred kilometers distance. The result should be dimensionless by dividing by the total test distance and expressed in terms of the cumulative height increase (m) per hundred kilometers distance.

Table 5 shows the statistical results of cumulative positive elevation increment and cumulative negative elevation increment for the whole trip of the six PEMS tests. Tables 6–8 show the statistical results of the cumulative positive elevation increment and cumulative negative elevation increment for the urban, suburban, and highway sections of the six

PEMS tests. The average values of the two test results for each route were used as the representative values of the cumulative elevation increment.

Table 5. Cumulative elevation increment statistics for the whole journey of 6 tests.

Item	Route 1		Route 2		Route 3	
	R1(1)	R1(2)	R2(1)	R2(2)	R3(1)	R3(2)
Cumulative positive elevation increment (m/100 km)	750.5	777.3	785.2	803.9	1062.1	1077.9
Average value (m/100 km)	763.9		794.5		1070.0	
Cumulative negative elevation increment (m/100 km)	−757.7	−764.7	−845.4	−841.9	−1277.8	−1057.2
Average value (m/100 km)	−761.2		−843.7		−1167.5	

Table 6. Cumulative elevation increment statistics of urban sections in 6 tests.

Item	Route 1		Route 2		Route 3	
	R1(1)	R1(2)	R2(1)	R2(2)	R3(1)	R3(2)
Cumulative positive elevation increment (m/100 km)	1209.7	1284.1	971.2	984.5	1210.9	1245.8
Average value (m/100 km)	1246.9		977.9		1228.4	
Cumulative negative elevation increment (m/100 km)	−1412.3	−1462.4	−2046.4	−2089.0	−2063.4	−2155.6
Average value (m/100 km)	−1437.3		−2067.7		−2109.5	

Table 7. Cumulative elevation increment statistics of suburban sections in 6 tests.

Item	Route 1		Route 2		Route 3	
	R1(1)	R1(2)	R2(1)	R2(2)	R3(1)	R3(2)
Cumulative positive elevation increment (m/100 km)	736.4	741.5	697.0	714.6	997.3	992.2
Average value (m/100 km)	739.0		705.8		994.8	
Cumulative negative elevation increment (m/100 km)	−553.2	−578.1	−809.1	−781.8	−1703.4	−1730.8
Average value (m/100 km)	−565.7		−795.4		−1717.1	

Table 8. Cumulative elevation increment statistics of highway sections in 6 tests.

Item	Route 1		Route 2		Route 3	
	R1(1)	R1(2)	R2(1)	R2(2)	R3(1)	R3(2)
Cumulative positive elevation increment (m/100 km)	457.5	407.1	731.8	762.6	1017.9	1040.4
Average value (m/100 km)	432.3		747.2		1029.1	
Cumulative negative elevation increment (m/100 km)	−962.6	−911.6	−756.7	−770.5	−1686.7	−1677.8
Average value (m/100 km)	−937.1		−763.6		−1682.3	

As can be seen from Table 5, following the order of Route 1, Route 2, and Route 3, the cumulative positive elevation increment shows a trend of sequentially increasing. The absolute value of the cumulative negative elevation increment also shows a trend of gradually increasing. This indicates that from Route 1 to Route 3, both the uphill and downhill amounts in the test are becoming larger and larger. In addition, the difference in cumulative positive elevation increment between Route 1 and Route 2 is relatively small, only differing by 30.6 m/100 km. The difference in cumulative positive elevation increment between Route 3 and both Route 1 and Route 2 is larger, being higher than Route 1 and Route 2 by 306.1 m/100 km and 275.5 m/100 km, respectively. In addition, the difference in cumulative positive elevation increment between Route 1 and Route 2 is small, with a difference of only 30.6 m/100 km. The cumulative elevation increment of Route 3 is larger than that of Route 1 and 2, which is higher than that of Route 1 and Route 2 by 306.1 m/100 km and 275.5 m/100 km, respectively.

Table 5 also shows that the absolute value difference between the cumulative negative elevation increment and the cumulative positive elevation increment is relatively small. For instance, in Route 1, the difference between the cumulative positive elevation increment and the cumulative negative elevation increment is only 2.8 m/100 km, while the largest difference is 97.5 m/100 km in Route 3. This indicates that there is not much difference in the amount of uphill and downhill during PEMS tests on the three routes. This is because the PEMS test stipulates that the difference in elevation between the starting point and the ending point of the test road must not exceed 100 m. It also demonstrates that the parameter of cumulative negative elevation increment can effectively reflect the road slope characteristics in real road tests. The test results of Murena et al. (2019) [32] indicate that the fuel consumption penalty of uphill is not offset by the benefit of downhill. Therefore, it is necessary to propose the "cumulative negative elevation increment" indicator, which combines the characteristics of uphill and downhill, and to comprehensively analyze the impact of slope on fuel consumption and emissions through the method of combining uphill and downhill features on roads. Moreover, the pollutant emissions during the downhill phase of driving also need to be effectively controlled. Therefore, the indicator of the cumulative negative elevation increment may become an important limiting index in emission regulations in the future.

From Tables 6–8, it can be observed that in the order of Route 1, Route 2, and Route 3, the cumulative positive elevation increment of the urban and suburban sections and the cumulative negative elevation increment of the highway section all decrease first and then increase, and the other cumulative positive and negative elevation increments all increase. This indicates that the characteristics of slope change in different sections of the three routes are not entirely consistent with those of the whole trip.

Moreover, the cumulative negative elevation increment in the urban section of Route 2 is approximately twice that of the cumulative positive elevation increment, and the cumulative negative elevation increment in the highway section of Route 1 is more than twice that of the cumulative positive elevation increment. This suggests significant differences in the amount of uphill and downhill slopes at each road section. It also shows a large difference in the slope characteristics between each road section and the whole trip.

Based on the driving power balance equation, the fuel consumption and emission change characteristics of different sections of the three routes are also not entirely consistent with those of the entire trip. Therefore, in order to obtain more accurate correlations between slope and fuel consumption and emission, it is necessary to count the slope characteristics by road sections and study the fuel consumption and emission characteristics of different routes by road sections.

Comparing the cumulative elevation increment for the urban, suburban, and highway segments of each trip in Tables 6–8, it is found that the cumulative elevation increments during the urban phase of the three routes are the highest, while those in the suburban and highway sections are relatively smaller. This indicates that there are more uphill and downhill sections in the urban phase of the three routes, while the roads in the suburban and highway phases are relatively flat, with fewer uphill and downhill sections. This is because all PEMS tests start from the urban area of Chongqing, where the terrain is more complex. As shown in the table, the cumulative positive elevation increments of Route 1 and Route 3 in the urban phases are greater than 1200 m/100 km, and the cumulative negative elevation increments of Route 2 and Route 3 in the urban phases even exceed 2000 m/100 km. The cumulative positive elevation increments of the three routes in suburban and highway sections are generally within the range of 1200 m/100 km.

3.2.2. Correlation Between Road Slope and Fuel Consumption

Whole Trip Level

Based on the test data, the total fuel consumption, specific fuel consumption, and fuel consumption factor (fuel consumption per unit of distance) of the six PEMS tests along the three experimental routes for the whole trip were counted. The results are shown in Figure 5. Figure 6 presents the cumulative engine work done along the entire route and each section of different routes.

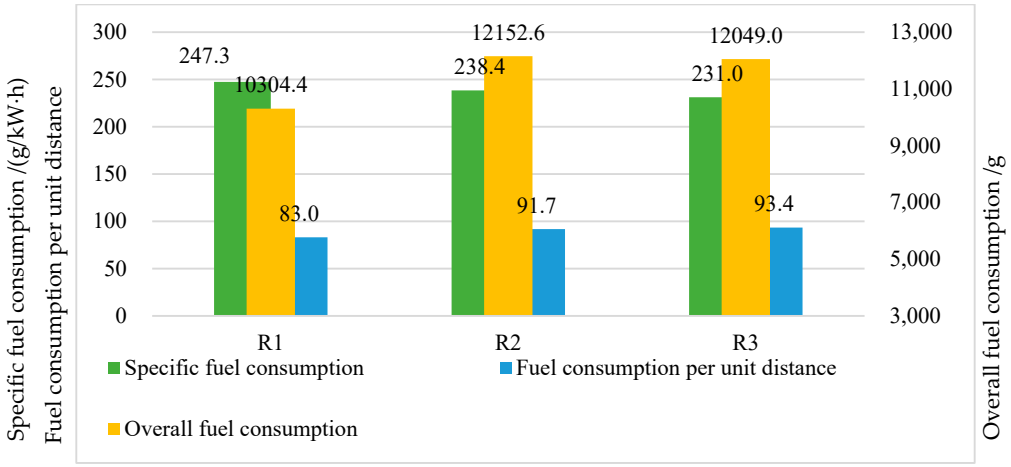

Figure 5. Total fuel consumption, specific fuel consumption, and fuel consumption per unit distance of the whole trip.

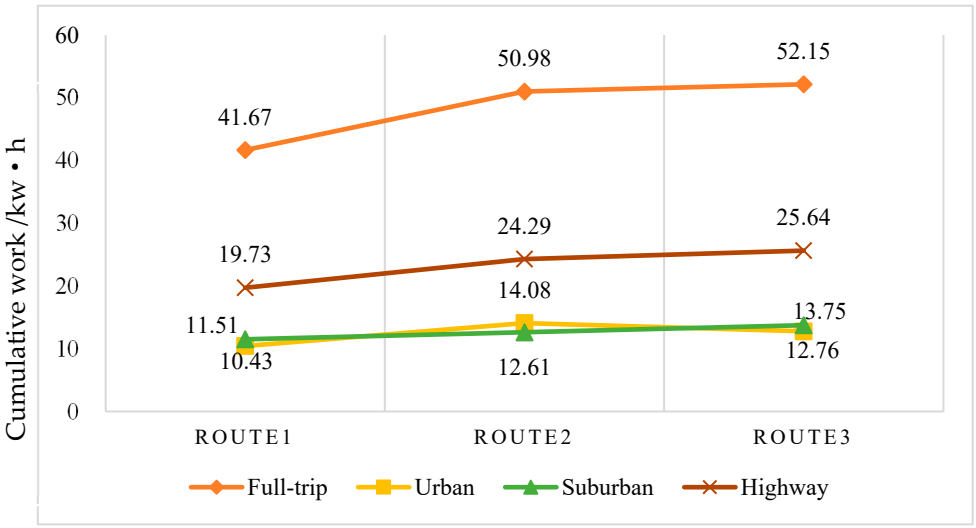

Figure 6. Cumulative work of total travel and each road section of different routes.

Figure 5 shows that, in the order of Route 1, Route 2, and Route 3, the fuel consumption factor increases sequentially. This indicates a positive correlation between the variations in fuel consumption factor and the slope of heavy-duty vehicles. This can be attributed to the differences in road conditions across the various routes, resulting in varying work done by the test vehicle. Based on the work data provided in Figure 6 and the distance information in Table 2, the work done per unit distance for Routes 1, 2, and 3 is calculated to be 0.336, 0.385, and 0.404 (kW·h), respectively. It is evident that as the work done per unit distance increases, the fuel consumption factor also increases. The increase in slope will cause an increase in work per unit distance, so the greater the slope, the greater the fuel consumption factor. This result is in accordance with the findings of Zachiotis and

Giakoumis [35] and Boriboonsomsin and Barth [27]. The greater the slope, the higher the fuel consumption.

Figure 5 also shows that the rates of change in fuel consumption factor on three routes do not coincide with the rate of change in slope. For instance, compared to Route 1, Route 2 has a 4% increase in slope but a 10.5% increase in the fuel consumption factor; whereas, compared to Route 2, Route 3 has a 34.7% increase in slope but only a 1.9% increase in the fuel consumption factor. Overall, when the change rate of slope is small, the change rate of fuel consumption is large. It is necessary to further analyze the underlying reasons from the perspective of road sections, combining the characteristics of the cumulative positive and negative elevation increment.

When comparing the specific fuel consumption of the three routes, it is observed that as the slope increases, the specific fuel consumption decreases, indicating a deterioration in fuel efficiency. Total fuel consumption is related to both specific fuel consumption and route length.

Road Section Level

Figure 7 shows that changes in total fuel consumption, fuel consumption factor, and specific fuel consumption on the urban sections of the three routes are not significantly correlated with changes in road slope. The total fuel consumption, fuel consumption factor, and specific fuel consumption on Route 2 are all the highest. And Figure 6 also reflects that the work done by the engine on Route 2 is also the largest.

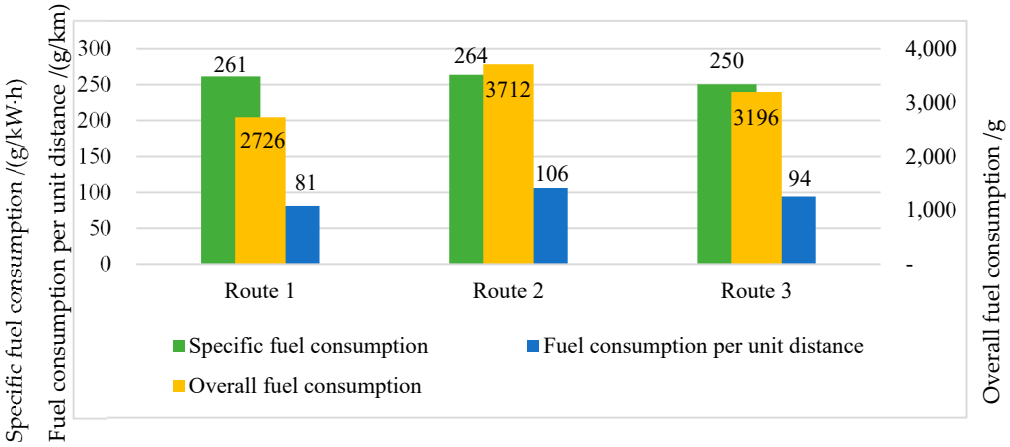

Figure 7. Statistical chart of total fuel consumption, specific fuel consumption, and fuel consumption per unit distance of urban travel.

Comparing Route 1 with Route 2, the positive elevation increment of Route 2 is less than that of Route 1. Based on the driving dynamics theory and ignoring the differences in driving dynamic characteristics, theoretically, the fuel consumption of the uphill section on Route 2 should be less than that on Route 1. At the same time, the downhill amount of Route 2 is larger than that of Route 1; theoretically, the fuel consumption of the downhill section on Route 2 should be less than that on Route 1. However, test data show that the fuel consumption on Route 2 is greater than that on Route 1, indicating that the impact of driving dynamics factors (such as speed, acceleration, etc.) cannot be ignored. Comparing the dynamic parameters on the urban section, the positive driving forces on Routes 1 and 2 are, respectively, 0.35 m^2/s^3 and 0.52 m^2/s^3. It can be seen that the positive driving force on Route 2 is higher than that on Route 1. Based on the theory of driving dynamics, this will increase the fuel consumption on Route 2. Since the experiment was driven by the same driver, the main factors causing differences in dynamic characteristics should be road slope and urban traffic factors.

Similarly, comparing Route 2 with Route 3, the positive elevation increment of Route 3 is significantly greater than that of Route 2. Ignoring the differences in driving dynamics characteristics, the fuel consumption on Route 3 should be significantly higher than that on Route 2. The negative elevation increment of Route 3 is slightly greater than that of Route 2, and fuel consumption on Route 3 should be slightly lower than that on Route 2. Therefore, theoretically, the fuel consumption on Route 3 should be higher than that on Route 2. However, test data show that the fuel consumption on Route 3 is less than that on Route 2, also revealing that the impact of driving dynamics factors on fuel consumption cannot be ignored. Comparing the dynamic parameters on the urban section, the positive driving force on Routes 2 and 3 are, respectively, 0.52 m^2/s^3 and 0.44 m^2/s^3. It can be seen that the positive driving force on Route 2 is higher than that on Route 3. Based on the theory of driving dynamics, this will increase the fuel consumption on Route 2.

Figure 8 shows that the changes in total fuel consumption and fuel consumption factor on the suburban sections of the three routes are positively correlated with changes in the cumulative negative elevation increment but not significantly correlated with changes in the positive elevation increment. The specific fuel consumption on Route 2 is the highest.

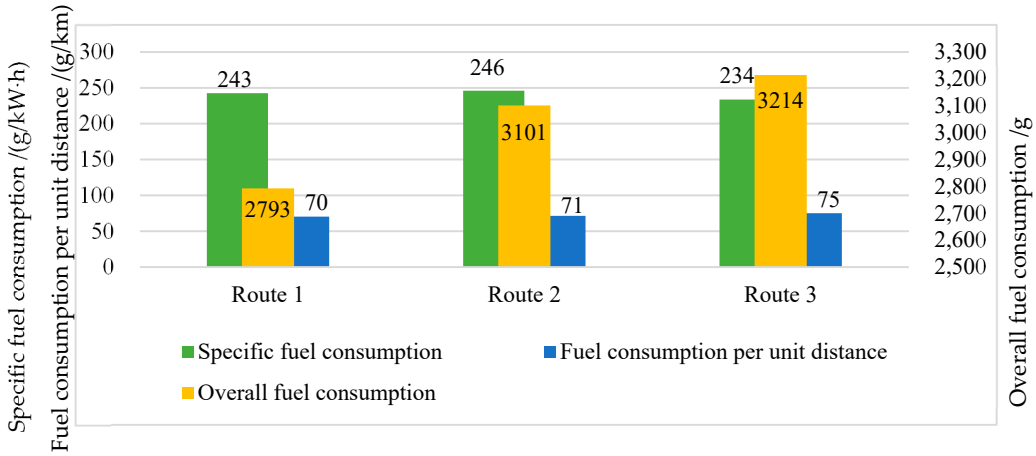

Figure 8. Statistical chart of total fuel consumption, specific fuel consumption, and fuel consumption per unit distance of suburban travel.

Comparing Route 1 with Route 2, the positive elevation increment of Route 2 is less than that of Route 1. Based on the driving dynamics theory and ignoring the differences in driving dynamics, theoretically, the fuel consumption on the uphill section of Route 2 is less than that on Route 1. Meanwhile, the negative elevation increment of Route 2 is greater than that of Route 1; theoretically, the fuel consumption on the downhill section of Route 2 is less than that on Route 1. However, test data show that the fuel consumption on Route 2 is greater than that on Route 1, indicating that the impact of driving dynamic factors cannot be ignored. Since the experiment was driven by the same driver, the main factor causing differences in dynamic characteristics should be the road slope. Comparing the dynamic parameters on the suburban section, the positive driving force on Routes 1 and 2 are, respectively, 0.52 m^2/s^3 and 0.61 m^2/s^3. It can be seen that the positive driving force on Route 2 is higher than it is on Route 1. Based on the theory of driving dynamics, this will increase the fuel consumption on Route 2.

Figure 9 shows that the changes in total fuel consumption and fuel consumption factor on the highway sections of the three routes are positively correlated with the changes in cumulative positive elevation increment but not significantly correlated with changes in negative elevation increment. The specific fuel consumption on Route 1 is the highest. It

can be seen that the traffic conditions on the highway section are good, and the main factor affecting the fuel consumption is the slope.

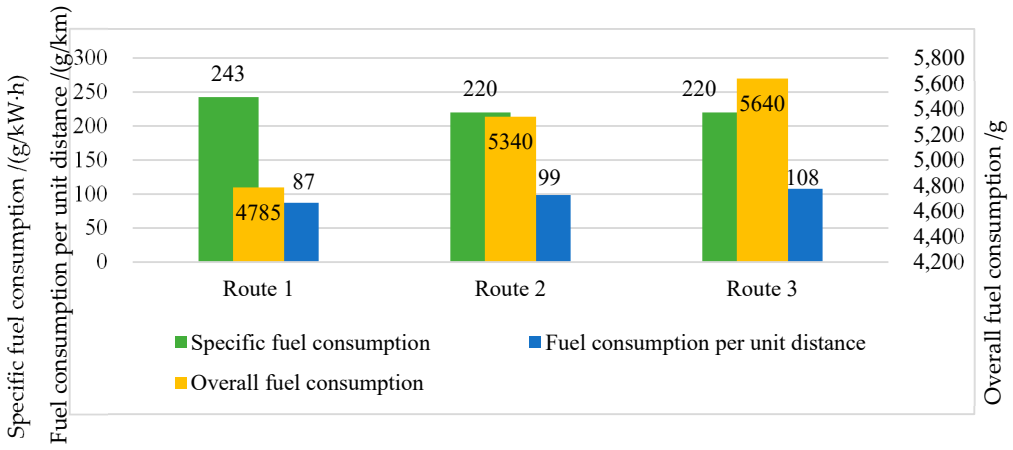

Figure 9. Statistical chart of total fuel consumption, specific fuel consumption, and fuel consumption per unit distance of high-speed travel.

3.2.3. Correlation Between Road Slope and Pollutant Emissions

According to the China National VI emission regulations for heavy-duty commercial vehicles, the power-based window method is used for the statistical analysis of various pollutant emission factors at the full-trip level. In each route, the average value of the emission factors of two tests is taken as the final emission result. Figure 10 shows the actual pollutant emission results of heavy-duty diesel vehicles on three routes.

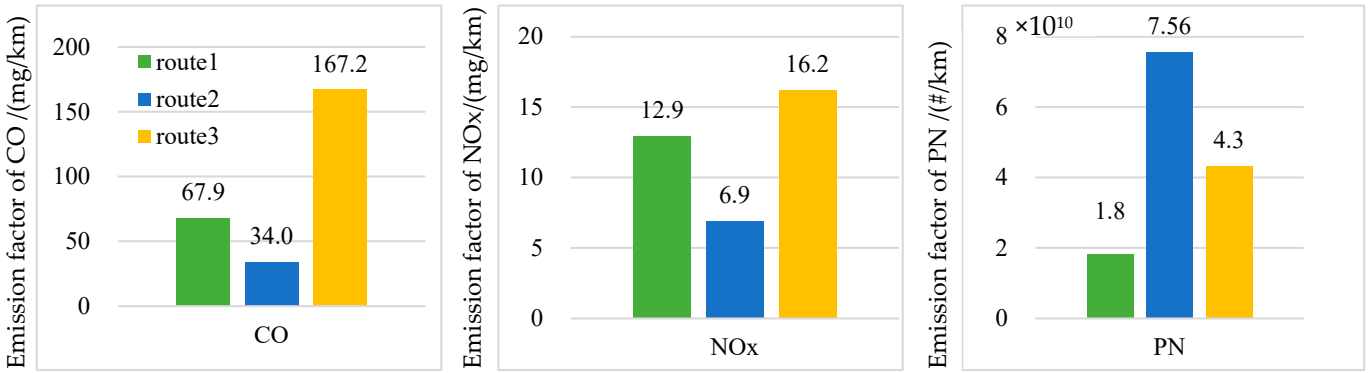

(**a**) CO (**b**) NO_X (**c**) PN

Figure 10. Total trip emission results of pollutants in different routes.

Whole Trip Level

Figure 10a–c show that on comparing Route 1 and Route 3, as the slope increases, CO, NO_X, and PN all increase. It can be seen that the changes in CO, NO_X, and PN emissions show a positive correlation with the change in slope. Comparing Route 1 and Route 2, as the slope increases, CO and NO_X decrease instead. Comparing Route 2 and Route 3, as the slope increases, PN decreases instead.

CO is a product of incomplete combustion, and both rich combustion and low temperatures will lead to incomplete combustion. The average engine coolant temperature on all three routes was between 351.5 and 352 K during the tests (see Table 9), so the influence of temperature factors on engine emissions is excluded here. Therefore, the amount of CO mainly depends on the fuel consumption and rich combustion conditions. According to the engine load–fuel consumption relationship, when the engine is under heavy load, a rich

combustion condition occurs, leading to the production of incomplete combustion product CO. According to the power balance equation, when the slope of the road increases, the engine load and rich combustion condition increase, resulting in an increase in CO emission. At the same time, rich combustion conditions increase. Together, these two changes lead to an increase in CO. However, the test CO on Route 2 decreased compared to Route 1, and the reason for this needs further analysis. Additionally, during testing, the exhaust gas temperature on Route 2 was 18.7 higher than the average exhaust gas temperature on Route 1 (see Table 9), which improved the CO conversion efficiency of the after-treatment device and reduced CO on Route 2.

Table 9. Test engine coolant temperature and exhaust temperature.

Item	Route 1	Route 2	Route 3
Average temperature of engine coolant/K	351.6	351.9	351.8
Average exhaust temperature/K	485.6	504.3	497.5

It is generally accepted that high temperatures and hypoxic conditions lead to the generation of PN. Generally speaking, as the slope increases, the engine load increases, and the engine output power increases, which is prone to high-temperature and rich combustion conditions, thus leading to an increase in PN. However, the test PN on Route 3 decreased compared to Route 2. The relative positive accelerations on Routes 2 and 3 were 0.05 m/s^2 and 0.045 m/s^2, respectively. As can be seen, the variation of driving state during the test on Route 2 was more intense, which could have led to the production of black smoke, thereby increasing the PN level on Route 2.

It is generally believed that the NO_X produced at high temperatures accounts for the majority of the NO_X generated by engines. The cumulative elevation increment of Route 2 is larger than that of Route 1, theoretically implying more high-temperature conditions on Route 2, and thus, the NO_X on Route 2 should be higher than that of Route 1. However, test data results contradict this expectation. During testing, there was no significant difference in the working temperature of the engines across the three routes, but Table 9 shows that the average exhaust temperature on Route 2 is 18.7 K higher than that on Route 1 and 6.8 K higher than that on Route 3. It is possible that the after-treatment device on Route 2 has the highest conversion efficiency for NO_X, thereby reducing its levels. Additionally, driving dynamics factors may also have some impact on NO_X production.

It is evident that the research based on the level of the whole trip reveals parts of the correlation mechanisms between slope and emissions. However, there are still some unclear correlations. It is necessary to conduct a comprehensive research study based on the level of road segment by combining positive and negative elevation characteristics on road sections to further elucidate the correlation mechanism between slope and emissions and to clarify whether driving dynamics factors play a role.

Road Section Level

Figure 11 shows that compared to Route 1, all emissions on urban, suburban, and highway sections of Route 3 increase with increasing slope. This result is in accordance with the results found in the literature [32,35]. The greater the slope, the greater the pollutant emissions.

Comparing Route 1 and Route 2, the changes in CO on urban, suburban, and highway sections show a positive correlation with changes in cumulative positive elevation increment. Compared to Route 1, the cumulative positive elevation increments on the urban and suburban sections of Route 2 decrease, reducing engine load and rich combustion conditions, which, in turn, reduces the production of incomplete combustion product CO. In contrast, the cumulative positive elevation increment on the highway section of Route 2

increases compared to Route 1, ultimately leading to an increase in CO. Compared to Route 2, the cumulative positive elevation increment on urban, suburban, and highway sections of Route 3 all increase, and CO on corresponding road sections all increase. Here, statistical data show that the differences in the average value of engine coolant temperature on urban, suburban, and highway sections across the three routes do not exceed 0.5 °C, eliminating the influence of engine temperature on CO. The exhaust gas temperatures on each section of Route 2 are slightly higher than those of Route 1, with the maximum difference being less than 10%. It is possible that the conversion efficiency of the after-treatment device on Route 2 is slightly higher, reducing a portion of CO.

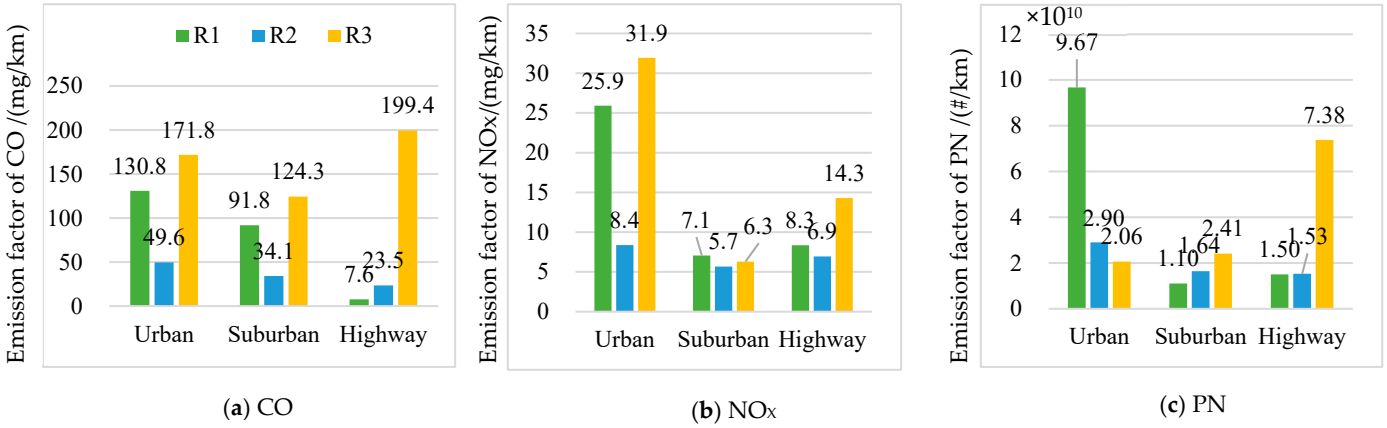

(**a**) CO (**b**) NOx (**c**) PN

Figure 11. Emission results of pollutants in different road sections.

From the analysis above, it can be seen that as the slope increases, both rich combustion conditions and temperature increase, resulting in an increase in PN. However, Figure 11c shows that PN emission on the urban section of Route 2 is the highest, but its cumulative positive elevation increment is the smallest. It is noted that the driving force on the urban section of Route 2 is higher than that of Routes 1 and 3, indicating that intense changes in driving dynamics have led to a significant increase in PN. The cumulative elevation increment on the highway section of Route 3 is greater than that of Route 2, yet the PN on this section of Route 2 is abnormally high, suggesting that driving dynamics may have affected the production of PN. The cumulative elevation increment on the suburban section of Route 2 is lower than that of Route 1, and according to the previous analysis, the driving force of Route 2 is higher than that of Route 1, so the PN on this road section is instead higher than that on Route 1. Therefore, it can be seen that the impact of driving dynamics factors has led to a significant increase in PN on some sections.

Comparing Route 1 and Route 2, the changes in NO_X on urban and suburban sections show a positive correlation with the changes in cumulative positive elevation increments. Compared to Route 1, the cumulative positive elevation increments on the urban and suburban sections of Route 2 decrease, reducing engine load and NO_X produced at high temperatures. However, compared to Route 1, the cumulative positive elevation increment on the highway section of Route 2 increases, but NO_X does not increase. Here, the exhaust temperature of the engine on Route 2 is slightly higher than that on Route 1, so we speculate that exhaust gas temperature and driving dynamics factors combine to cause the NO_X on the highway section of Route 2 to be lower than that on Route 1. Compared to Route 2, the cumulative positive elevation increments on the urban, suburban, and highway sections of Route 3 all increase, increasing engine load and NO_X produced at high temperatures.

4. Conclusions

This research proposes a method of using cumulative positive and negative elevation increment indicators based on road segment to identify the slope characteristics of mountain city roads. Furthermore, it is proposed to use the aforementioned indicators, based on the theory of driving dynamics and emission theory, to analyze the correlation characteristics and inherent correlation mechanism between the slope of mountain city roads and the actual driving fuel consumption and emissions. For this purpose, we conducted real-world driving fuel consumption and emission tests for heavy-duty diesel vehicles on typical mountain city roads in Chongqing, China, and carried out comprehensive and in-depth research on driving fuel consumption and emission characteristics.

- The differences in specific fuel consumption and pollutant emissions are minimal in the three C-WTVC cycle tests under laboratory conditions, and this result is also observed in the two PEMS tests on a real-world road. This indicates that as long as the tests are conducted in accordance with regulatory requirements, the repeatability of both the PEMS test on real-world routes and the C-WTVC cycle test under laboratory conditions can be controlled. Road slope causes the specific fuel consumption and specific emissions in the PEMS test to be higher than those in the C-WTVC cycle test, with the former being 6.8% higher in specific fuel consumption and a larger difference in specific emission.
- The cumulative positive and negative elevation increment indicators calculated based on road segment can correctly identify the complex slope characteristics of mountain city roads. At the level of the whole trip, the cumulative positive and negative elevation increments increase, in turn, in the order of Route 1, Route 2, and Route 3, but the slope changes in trip road sections are not completely consistent with the whole-trip slope change across the three routes. And there is a significant difference between the cumulative positive and negative elevation increments of the road section. It is necessary to propose the "cumulative negative elevation increment" indicator to study the impact of downhill on actual driving and to comprehensively analyze the impact of road slope on fuel consumption and emissions.
- Using the cumulative positive and negative elevation increment index, the research method based on driving dynamics and emission theory successfully reveals correlation characteristics and inherent mechanisms between the slope of mountain city roads and the actual fuel consumption and emissions of heavy-duty diesel vehicles.
- Overall, the change in fuel consumption factor is positively correlated with the change in slope, but the specific rate of change is not consistent. Compared to Route 1, the slope of Route 2 increased by 4%, but the fuel consumption factor on Route 2 increased by 10.5%. Compared to Route 2, the slope of Route 3 increased by 34.7%, but the fuel consumption factor on Route 3 only increased by 1.9%. The inconsistent rate of change is mainly related to driving dynamics. The study further reveals the intrinsic influence mechanism of slope on fuel consumption: an increase in slope causes an increase in required power, thereby leading to an increase in fuel consumption. In addition, changes in driving dynamics also affect fuel consumption. When studying the correlation between slope and fuel consumption, the impact of driving dynamics factors cannot be ignored.
- The changes in pollutants CO, NO_X, and PN are positively correlated with the changes in slope. The research further reveals the intrinsic impact mechanism of slope on pollutants: an increase in slope leads to an increase in load, thereby increasing the required fuel consumption and rich combustion conditions, ultimately leading to an increase in pollutants. In addition, changes in driving dynamics also affect emissions,

significantly increasing the PN on some road sections. In addition, exhaust gas temperature may have a certain impact on emissions.

- This research elucidates the relationship and correlation mechanism between the road slope of mountain city roads and fuel consumption and emissions, providing a foundation for the development of fuel consumption and emission prediction. It also lays the groundwork for the formulation of energy-saving and emission-reduction driving strategies, enabling ecological and energy-efficient driving for motor vehicles, thereby supporting sustainable social development.

Author Contributions: G.T.: Methodology, Investigation, Data curation, Writing—review and editing, Validation, Project administration, Funding acquisition. D.L.: Conceptualization, Methodology, Test, Data curation, Writing—original draft. J.L.: Conceptualization, Methodology, Validation. X.D.: Test, Data curation. All authors have read and agreed to the published version of the manuscript.

Funding: This work was supported by the Natural Science Foundation General Project of Chongqing Municipal: [Grant No. CSTB2022NSCQ-MSX1359].

Institutional Review Board Statement: Not applicable.

Informed Consent Statement: Not applicable.

Data Availability Statement: Data will be available on reasonable request.

Conflicts of Interest: The authors declare that they have no known competing financial interests or personal relationships that could have appeared to influence the work reported in this paper.

Abbreviations

The following abbreviations are used in this manuscript:

CO	carbon monoxide
CO_2	carbon dioxide
NO_X	nitrogen oxides
PN	Particulate Number
PM	Particulate Matter
PEMS	Portable Emission Measurement System
SCR	Selective Catalytic Reduction
LiDAR	Light Detection And Ranging
GIS	Geographic Information System
PHEM	Passenger Car and Heavy-Duty Emission Model
GPS	Global Positioning System
NREL	National Renewable Energy Laboratory
RMS	Root Mean Square
WHTC	World Harmonized Transient Cycle
C-WTVC	Adapted World Transient Vehicle Cycle
EGR	Exhaust Gas Recirculation
DOC	Diesel Oxidation Catalyst
ASC	Ammonia Slip Catalyst
DPF	Diesel Particulate Filter
EFM	Exhaust Flow Meter
NDUV	Non-dispersive Ultraviolet
NDIR	Non-dispersive infrared
DC	direct current
OBD	On-Board Diagnostics
RPA	relative positive acceleration

References

1. National Bureau of Statistics of the People's Republic of China. *China Statistical Yearbook 2021*; China Statistics Press: Beijing, China, 2021.
2. Zheng, H.; Zhao, B.; Wang, S.; Wang, T.; Ding, D.; Chang, X.; Liu, K.; Xing, J.; Dong, Z.; Aunan, K.; et al. Transition in source contributions of PM2.5 exposure and associated premature mortality in China during 2005–2015. *Environ. Int.* **2019**, *132*, 105111. [CrossRef]
3. Cary, M.; Ahmed, Z. Do heavy-duty and passenger vehicle emissions standards reduce per capita emissions of oxides of nitrogen? *Evid. Eur. Environ. Manag.* **2022**, *320*, 115786. [CrossRef] [PubMed]
4. Yang, D.; Zhang, S.; Niu, T.; Wang, Y.; Xu, H.; Zhang, K.M.; Wu, Y. High-resolution mapping of vehicle emissions of atmospheric pollutants based on large-scale, real-world traffic datasets. *Atmos. Chem. Phys.* **2019**, *19*, 8831–8843. [CrossRef]
5. Wang, J.; Wang, R.; Yin, H.; Wang, Y.; Wang, H.; He, C.; Liang, J.; He, D.; Yin, H.; He, K. Assessing heavy-duty vehicles (HDVs) on-road NOx emission in China from on-board diagnostics (OBD) remote report data. *Sci. Total Environ.* **2022**, *846*, 157209. [CrossRef] [PubMed]
6. Zhang, S.; Zhao, P.; He, L.; Yang, Y.; Liu, B.; He, W.; Cheng, Y.; Liu, Y.; Liu, S.; Hu, Q.; et al. On-board monitoring (OBM) for heavy-duty vehicle emissions in China: Regulations, early-stage evaluation and policy recommendations. *Sci. Total Environ.* **2020**, *731*, 139045. [CrossRef]
7. Zhang, J.; Xia, C.; Wang, H.; Tang, C. Recent advances in electrocatalytic oxygen reduction for on-site hydrogen peroxide synthesis in acidic media. *J. Energy Chem.* **2021**, *67*, 432–450. [CrossRef]
8. Borucka, A.; Wiśniowski, P.; Mazurkiewicz, D.; Świderski, A. Laboratory measurements of vehicle exhaust emissions in conditions reproducing real traffic. *Measurement* **2021**, *174*, 108998. [CrossRef]
9. Pavlovic, J.; Marotta, A.; Ciuffo, B. CO_2 emissions and energy demands of vehicles tested under the NEDC and the new WLTP type approval test procedures. *Appl. Energy* **2016**, *177*, 661–670. [CrossRef]
10. Wang, S.; Li, Y.; Fu, J.; Liu, J.; Dong, H. Numerical research on the performance, combustion and energy flow characteristics of gasoline-powered vehicle under WLTC. *Fuel* **2021**, *285*, 119135. [CrossRef]
11. Wang, X.; Ge, Y.; Gong, H.; Yang, Z.; Tan, J.; Hao, L.; Su, S. Ammonia emissions from China-6 compliant gasoline vehicles tested over the WLTC. *Atmos. Environ.* **2019**, *199*, 136–142. [CrossRef]
12. Li, T.; Chen, X.; Yan, Z. Comparison of fine particles emissions of light-duty gasoline vehicles from chassis dynamometer tests and on-road measurements. *Atmos. Environ.* **2013**, *68*, 82–91. [CrossRef]
13. Luján, J.M.; Bermúdez, V.; Dolz, V.; Monsalve-Serrano, J. An assessment of the real-world driving gaseous emissions from a Euro 6 light-duty diesel vehicle using a portable emissions measurement system (PEMS). *Atmos. Environ.* **2018**, *174*, 112–121. [CrossRef]
14. European Commission. *Commission Regulation (EU) 2017/1151 of 1 June 2017 Supplementing Regulation (EC) No 715/2007 of the European Parliament and of the Council on Type-Approval of Motor Vehicles with Respect to Emissions from Light Passenger and Commercial Vehicles (Euro 5 a. Off. J. Eur. Union 1–643)*; European Commission: Brussels, Belgium, 2017.
15. Triantafyllopoulos, G.; Dimaratos, A.; Ntziachristos, L.; Bernard, Y.; Dornoff, J.; Samaras, Z. A study on the CO_2 and NOx emissions performance of Euro 6 diesel vehicles under various chassis dynamometer and on-road conditions including latest regulatory provisions. *Sci. Total Environ.* **2019**, *666*, 337–346. [CrossRef] [PubMed]
16. Liu, H.; Barth, M.; Scora, G.; Davis, N.; Lents, J. Using portable emission measurement systems for transportation emissions studies. *Transp. Res. Rec. J. Transp. Res. Board* **2010**, *2158*, 54–60. [CrossRef]
17. Gallus, J.; Kirchner, U.; Vogt, R.; Börensen, C.; Benter, T. On-road particle number measurements using a portable emission measurement system (PEMS). *Atmos. Environ.* **2016**, *124*, 37–45. [CrossRef]
18. Seo, J.; Park, J.; Park, J.; Park, S. Emission factor development for light-duty vehicles based on real-world emissions using emission map-based simulation. *Environ. Pollut.* **2021**, *270*, 116081. [CrossRef]
19. Degraeuwe, B.; Weiss, M. Does the New European Driving Cycle (NEDC) really fail to capture the NOX emissions of diesel cars in Europe? *Environ. Pollut.* **2017**, *222*, 234–241. [CrossRef] [PubMed]
20. Guor, S.; Zhang, Y.; Cai, G.Q. Study on exhaust emission test of diesel vehicles based on PEMS. *Procedia Comput. Sci.* **2020**, *166*, 428–433. [CrossRef]
21. Li, X.; Ai, Y.; Ge, Y.; Qi, J.; Feng, Q.; Hu, J.; Porter, W.C.; Miao, Y.; Mao, H.; Jin, T. Integrated effects of SCR, velocity, and Air-fuel Ratio on gaseous pollutants and CO_2 emissions from China V and VI heavy-duty diesel vehicles. *Sci. Total Environ.* **2022**, *811*, 152311. [CrossRef] [PubMed]
22. Xia, Y.; Liao, C.; Chen, X.; Zhu, Z.; Chen, X.; Wang, L.; Jiang, R.; Stettler ME, J.; Angeloudis, P.; Gao, Z. Future reductions of China's transport emissions impacted by changing driving behaviour. *Nat. Sustain.* **2023**, *6*, 1228–1236. [CrossRef]
23. Lois, D.; Wang, Y.; Boggio-Marzet, A.; Monzon, A. Multivariate analysis of fuel consumption related to eco-driving: Interaction of driving patterns and external factors. *Transp. Res. Part D Transp. Environ.* **2019**, *72*, 232–242. [CrossRef]

24. Zhai, Z.; Tu, R.; Xu, J.; Wang, A.; Hatzopoulou, M. Capturing the variability in instantaneous vehicle emissions based on field test data. *Atmosphere* **2020**, *11*, 765. [CrossRef]
25. Fontaras, G.; Zacharof, N.; Ciuffo, B. Fuel consumption and CO_2 emissions from passenger cars in Europe—Laboratory versus real-world emissions. *Prog. Energy Combust. Sci.* **2017**, *60*, 97–131. [CrossRef]
26. Costagliola, M.A.; Costabile, M.; Prati, M.V. Impact of road grade on real driving emissions from two Euro 5 diesel vehicles. *Appl. Energy* **2018**, *231*, 586–593. [CrossRef]
27. Boriboonsomsin, K.; Barth, M. Impacts of road grade on fuel consumption and carbon dioxide emissions evidenced by use of advanced navigation systems. *Transp. Res. Rec. J. Transp. Res. Board* **2009**, *2139*, 21–30. [CrossRef]
28. Travesset-Baro, O.; Rosas-Casals, M.; Jover, E. Transport energy consumption in mountainous roads. A comparative case study for internal combustion engines and electric vehicles in Andorra. *Transp. Res. Part D Transp. Environ.* **2015**, *34*, 16–26. [CrossRef]
29. Zhang, W.; Lu, J.; Xu, P.; Zhang, Y. Moving towards Sustainability: Road Grades and On-Road Emissions of Heavy-Duty Vehicles—A Case Study. *Sustainability* **2015**, *7*, 12644–12671. [CrossRef]
30. Yang, H.; Dhital, N.B.; Cheruiyot, N.K.; Wang, L.; Wang, S. Effects of road grade on real-world tailpipe emissions of regulated gaseous pollutants and volatile organic compounds for a Euro 5 motorcycle. *Atmos. Pollut. Res.* **2021**, *12*, 101167. [CrossRef]
31. Wyatt, D.W.; Li, H.; Tate, J.E. The impact of road grade on carbon dioxide (CO_2) emission of a passenger vehicle in real-world driving. *Transp. Res. Part D Transp. Environ.* **2014**, *32*, 160–170. [CrossRef]
32. Murena, F.; Prati, M.V.; Costagliola, M.A. Real driving emissions of a scooter and a passenger car in Naples city. *Transp. Res. Part D Transp. Environ.* **2019**, *73*, 46–55. [CrossRef]
33. Lopp, S.; Wood, E.; Duran, A. Evaluating the impact of road grade on simulated commercial vehicle fuel economy using Real-World drive cycles. *SAE Tech. Pap.* **2015**. [CrossRef]
34. Wood, E.; Burton, E.; Duran, A.; Gonder, J. Contribution of road grade to the energy use of modern automobiles across large datasets of Real-World drive cycles. *SAE Tech. Pap.* **2014**. [CrossRef]
35. Zachiotis, A.T.; Giakoumis, E.G. Methodology to Estimate Road Grade Effects on Consumption and Emissions from a Light Commercial Vehicle Running on the WLTC Cycle. *J. Energy Eng.* **2020**, *146*, 04020048. [CrossRef]

Disclaimer/Publisher's Note: The statements, opinions and data contained in all publications are solely those of the individual author(s) and contributor(s) and not of MDPI and/or the editor(s). MDPI and/or the editor(s) disclaim responsibility for any injury to people or property resulting from any ideas, methods, instructions or products referred to in the content.